Cooperative Jahn-Teller Effect in Titanium Alum

Philip L. W. Tregenna-Piggott,[†,‡,#] Stephen P. Best,[*,‡,§] Mary C. M. O'Brien,[⊥] Kevin S. Knight,[||] J. Bruce Forsyth,[||] and John R. Pilbrow[†]

Contribution from the Department of Physics, Monash University, Clayton, Victoria 3168, Australia, Department of Chemistry, University College London, 20 Gordon Street, London WC1H 0AJ, England, School of Chemistry, University of Melbourne, Parkville, Victoria 3052, Australia, Department of Physics, Theoretical Physics, University of Oxford, 1 Keble Road, Oxford OX1 3NP, England, and Neutron Science Division, Rutherford Appleton Laboratory, Chilton, Oxon OX11 0QX, England

Received October 7, 1996[⊗]

Abstract: A low-temperature (ca. 12 K) cubic ($Pa\bar{3}$) to orthorhombic (*Pbca*) phase transition of the β-alum $CsTi(SO_4)_2{\cdot}12H_2O$ has been characterized by High Resolution Powder Neutron Diffraction and EPR measurements. Single crystal Raman spectra of the corresponding rubidium alum, $RbTi(SO_4)_2{\cdot}12H_2O$, show that a phase transition from the β-alum structure also occurs over the temperature range 5−15 K, with the spectroscopic changes remarkably similar for the caesium and rubidium salts. The structural instability of the titanium(III) alums is not evident in the corresponding salts of larger or smaller tervalent cations and hence is interpreted in terms of the electronic structure of $[Ti(OH_2)_6]^{3+}$. It is proposed that in the high-temperature cubic phase the S_6 site symmetry lifts the degeneracy of the t_{2g} (O_h) orbitals to leave the e_g (S_6) orbital set lowest lying. The resultant ^2E_g (S_6) ground term is subject to Jahn-Teller coupling with E_g phonon modes. The phase transition is interpreted as arising from a long-range interaction between the Jahn-Teller centers in the lattice giving rise to a cooperative Jahn-Teller effect. The proposed electronic structure of $[Ti(OH_2)_6]^{3+}$ in $CsTi(SO_4)_2{\cdot}12H_2O$ is consistent with the framework used to describe other tervalent aqua ions but is at variance with the current interpretation—of 40 years standing—which was based on the premise that the site symmetry of the tervalent cation is retained at all temperatures. The long-standing problem of the anomalous ground state g values of $[Ti(OH_2)_6]^{3+}$ in $CsTi(SO_4)_2{\cdot}12H_2O$ ($g_{||} = 1.25$ and $g_{\perp} = 1.14$) is shown to arise as a consequence of the low symmetry distortion which results from a lowering of the site symmetry of $[Ti(OH_2)_6]^{3+}$ from S_6 ($Pa\bar{3}$) to C_i (*Pbca*).

1. Introduction

With a single 3d electron, $[Ti(OH_2)_6]^{3+}$ has served as the prototype for crystal field[1] and *ab initio* molecular orbital calculations of transition-metal complexes.[2] The titanium(III) hexaaqua cation, while oxidatively unstable, is sufficiently inert in the caesium sulfate alum, $CsTi(SO_4)_2{\cdot}12H_2O$ (CsTiSH), to permit spectroscopic and magnetochemical investigation. The salt is ideally suited for such studies being magnetically dilute ($r_{Ti-Ti} \approx 8.7$ Å) with high crystal ($Pa\bar{3}$) and site (S_6) symmetries.[3,4] Despite these factors, elucidation of the electronic structure of $[Ti(OH_2)_6]^{3+}$ in CsTiSH has remained elusive. The numerous models assume that the trigonal symmetry of the tervalent cation is retained over the whole experimental temperature range and that the trigonal field lowers the orbital degeneracy of the $^2T_{2g}$ (O_h) ground term to give an orbitally nondegenerate (^2A_g) ground term.[1,5−14] This interpretation appears to be inconsistent with that of the $3d^2$ cation, vanadium(III), where analysis of the magnetochemistry[15−18] and electronic spectroscopy[19−21] of the alums suggests that the the orbital degeneracy of the $^3T_{1g}$ (O_h) term is lifted by the trigonal field to give an orbitally nondegenerate ground term (^3A_g). Thus, the current interpretation of the electronic structure of $[Ti(OH_2)_6]^{3+}$ and $[V(OH_2)_6]^{3+}$ in the β-alum lattice requires that

* Author to whom correspondence should be addressed.
† Monash University.
‡ University College London.
§ University of Melbourne.
⊥ University of Oxford.
|| Rutherford Appleton Laboratory.
Present Address: Departement für Chemie und Biochemie, Universität Bern, Freiestrasse 3, Bern 9, CH-3000, Switzerland.

⊗ Abstract published in *Advance ACS Abstracts*, March 1, 1997.

(1) Van Vleck, J. H. *J. Chem. Phys.* **1939**, *7*, 61−71. Van Vleck, J. H. *J. Chem. Phys.* **1939**, *7*, 72−84.
(2) Tachikawa, H.; Ichikawa, T.; Yoshida, H. *J. Am. Chem. Soc.* **1990**, *112*, 982−987. Åkesson, R.; Pettersson, L. G. M.; Sandström, M.; Wahlgren, U. *J. Am. Chem. Soc.* **1994**, *116*, 8691−8704.
(3) Lipson, H. *Philos. Mag.* **1935**, *19*, 887. Lipson, H. *Proc. R. Soc. London, Ser. A*, **1935**, *151*, 347.
(4) Beattie, J. K.; Best, S. P.; Skelton, B. W.; White, A. H. *J. Chem. Soc., Dalton Trans.* **1981**, 2105−2111.
(5) Benzie, R. J.; Cooke, A. H. *Proc. R. Soc. London, Ser. A* **1951**, *209*, 269−278.
(6) Bleaney, B.; Bogle, G. S.; Cooke, A. H.; Duffus, R. J.; O'Brien, M. C. M.; Stevens, K. W. H. *Proc. Phys. Soc. London, Ser. A* **1955**, *68*, 57.
(7) Bose, A.; Chakravarty, A. S.; Chatterjee, R. *Proc. R. Soc. London, Ser A* **1960**, *255*, 145. Bose, A.; Chakravarty, A. S.; Chatterjee, R. *Indian J. Phys.* **1959**, *33*, 325. Dutta-Roy, S. K.; Chakravarty, A. S.; Bose, A. *Indian J. Phys.* **1959**, *33*, 483.
(8) Figgis, B. N.; Lewis, J.; Mabbs, F. E. *J. Chem. Soc.* **1963**, 2473.
(9) Gladney, H. M.; Swalen, J. D. *J. Chem. Phys.* **1965**, *42*, 1999.
(10) Mackinnon, J. A.; Bickerton, J. L. *Can. J. Phys.* **1970**, *48*, 814.
(11) Manoogian, A. *Can. J. Phys.* **1970**, *48*, 2577.
(12) Dionne, G. F. *Can. J. Phys.* **1972**, *50*, 2232.
(13) Shing, Y. H.; Walsh D. *Phys. Rev. Lett.* **1974**, *33*, 1067. Jesion, A.; Shing, Y. H.; Walsh, D. *Proceedings of the Eighteenth Ampere Congress*, Nottingham, England, Sept 9−14, 1974; Allen, P. S., Andrew, E. R., Bates, C. A., Eds.; University of Nottingham Press: Nottingham, England, 1975, p 561.
(14) Tachikawa, H.; Murakami, A. *J. Phys. Chem.* **1995**, *99*, 11046−11050.
(15) Van der Handel, J.; Siegert, *A. Physica* **1937**, *4*, 871.
(16) Fritz, J. J.; Pinch, H. L. *J. Am. Chem. Soc.* **1956**, *78*, 6223.
(17) Chakravarty, A. S. *Indian J. Phys.* **1958**, *32*, 447.
(18) Figgis, B. N.; Lewis, J.; Mabbs, F. E. *J. Chem. Soc.* **1960**, 2480.
(19) Best, S. P.; Clark, R. J. H. *Chem. Phys. Lett.* **1985**, *122*, 401−405.
(20) Hitchman, M. A.; McDonald, R. G.; Smith, P. W.; Stranger, R. *J. Chem. Soc., Dalton Trans*. **1988**, 1393−1395.
(21) Tregenna-Piggott, P. L. W.; Best, S. P. *Inorg. Chem.* **1996**, *35*, 5730−5736.

S0002-7863(96)03509-3 CCC: $14.00

the splitting of the one-electron orbitals of the t_{2g} orbital set be reversed for the respective ions. For the caesium β alums the $M^{III}O_6$ octahedron is regular and the neutron structures confirm that the mode of water coordination is trigonal planar.[22−25] Ligand field calculations suggest that the magnitude of the trigonal field splitting of vanadium(III) in the β alums is too large to be explained by a distortion of the $M^{III}O_6$ framework but requires an anisotropy in the metal−water π interaction.[20] It follows that the sign of the trigonal field depends on the orientation of the plane of the water molecule relative to the MO_6 framework together with the relative magnitudes of the metal−water interaction in and normal to the plane of the water molecule.[24] A difference in the ordering of the a_g and e_g (S_6) components of the t_{2g} orbitals therefore implies either a gross change in the orientation of the coordinated water molecule, with a concomitant change in the hydrogen bonding interactions, or a changeover in the relative magnitudes in the strength of the metal−water interaction in and normal to the plane of the ligand. We propose that neither of these explanations is tenable but that the basic assumption regarding the sign of the trigonal field for the titanium alum is in error.

The sulfate alums have the general formula $M^IM^{III}(SO_4)_2\cdot 12H_2O$ and occur in three modifications—α, β, and γ—all of which crystallize in the cubic space group $Pa\bar{3}$.[3,4,26] The β-alum modification occurs most generally when M^I is large, *e.g.* Cs, but also occurs with smaller monovalent cations when the tervalent cation has unequal occupancy of the t_{2g} orbitals (*e.g.* Ti[21,27] and V[21,27,28]). The hydrogen bonds which involve the water molecule coordinated to the highly polarizing M^{III} cation are the strongest in the lattice and these are important in determining the relative arrangements of the different groups within the structure. For the β alums the plane of the water molecule coordinated to M^{III} makes an angle of less than *ca.* 2° with the M^{III}−O bond vector and is rotated about the M−O bond vector by between 19 and 22°,[24] midway between that required for T_h and *all-horizontal* D_{3d} symmetry. The magnitude of the trigonal field is considerable, based on the splitting of the energies of the t_{2g} (O_h) orbitals for vanadium(III) determined directly ($^3E_g \leftarrow {}^3A_g$ electronic Raman band[19,21]) or indirectly (electronic spectra,[20] magnetochemistry[18]), and is too large to be attributed to distortion of the MO_6 framework. This implies a significant difference in the metal−water π interaction in and normal to the plane of the ligand (anisotropic metal−water π interaction). This interpretation was used to rationalize the near *all-horizontal* D_{3d} geometry of $[V(OH_2)_6]^{3+}$ lying on a site of C_i symmetry in the salt $[V(OH_2)_6][H_5O_2](CF_3SO_3)_4$[29] and the *all-vertical* D_{3d} geometry of $[Ti(OH_2)_6]^{3+}$ in the amorphous solid of a 2-propanol/D_2O mixture.[30] The most direct evidence for the anisotropic metal−water interaction derives from polarized neutron diffraction from $CsMo(SO_4)_2\cdot 12D_2O$,[31] which shows significant spin transfer normal to the plane of the ligand but no significant spin transfer in the metal−ligand plane. This result is consistent with simple considerations of the metal−ligand bonding.

The interpretation of the electronic structure of titanium(III) in CsTiSH has relied on the assumption that the metal site retains trigonal symmetry over the whole experimental temperature range. The ground state g values ($g_\parallel = 1.25$ and $g_\perp = 1.14$) for titanium(III) in CsTiSH[6] have been used to exclude the possibility that the trigonal field results in a ^2E_g ground term, since in this case the lowest lying Kramers doublet is predicted to be non-magnetic with $g_\parallel = 2(1 - k)$ and $g_\perp = 0$, k being the orbital reduction factor.[32] However, the argument against a ^2E_g ground term is not valid if the site symmetry of titanium(III) is reduced at low temperatures since in this instance both $g_\parallel$ and $g_\perp$ can be non-zero. Raman, EPR, and high-resolution powder neutron diffraction results are presented which permit characterization of a low-temperature phase transition of CsTiSH and identify an analogous phase transition of the corresponding rubidium salt. In both cases the structural instability is associated with the electronic structure of $[Ti(OH_2)_6]^{3+}$, where the trigonal field leaves an orbitally degenerate ground term for the d^1 cation. The $[Ti(OH_2)_6]^{3+}$ cations are subject to Jahn-Teller (JT) coupling with E_g lattice vibrations giving rise to a cooperative Jahn-Teller effect. The anomalous magnetochemistry and ground state g values for CsTiSH can be readily explained in the light of the phase transition. The significance of these results is to resolve the basic interpretation of the *simple* d^1 cation titanium(III) and, more importantly, to show that the interpretation of the electronic structure of metal hydrates is highly sensitive to metal−ligand π interactions and that these may be interpreted within a common framework.

2. Experimental Section

Large single crystals of CsTiSH and $RbTi(SO_4)_2\cdot 12H_2O$ (RbTiSH), suitable for single-crystal Raman spectroscopy, were grown from sulfuric acid (1 mol dm^{-3}) solutions of the appropriate salt using a thermal gradient technique described previously.[33,34] Deuterated samples of CsTiSH were prepared from repeated (3 times) recrystallization of the salt from $^2H_2SO_4$ (99 atom % ^2H). All solutions of titanium(III) were deoxygenated and handled under an atmosphere of dinitrogen or argon.

Raman spectra were obtained using a SPEX 14016 spectrometer in conjunction with a Burle GaAs 31034 photomultiplier tube with single photon counting. Excitation was provided by Coherent CR3000 K Kr^+ or I18 Ar^+ lasers. Low-temperature spectra were obtained using an Oxford instruments MD4 cryostat, the sample being maintained in a helium exchange gas. The temperature of the sample was estimated from the relative intensities of the Stokes and anti-Stokes Raman bands or, at liquid helium temperatures, from a Rh/Fe resistor attached to the sample holder. Details of the factor group analysis[33,35] and assignment of the Raman spectra of the alums[21,33−38] have been published previously.

(22) Best, S. P.; Forsyth, J. B. *J. Chem. Soc., Dalton Trans.* **1990**, 395−400.
(23) Best, S. P.; Forsyth, J. B. *J. Chem. Soc., Dalton Trans.* **1990**, 3507−3511.
(24) Best, S. P.; Forsyth, J. B. *J. Chem. Soc., Dalton Trans.* **1991**, 1721−1725.
(25) Best, S. P.; Forsyth, J. B.; Tregenna-Piggott, P. L. W. *J. Chem. Soc., Dalton Trans.* **1993**, 2711−2715.
(26) Armstrong, R. S.; Beattie, J. K.; Best, S. P.; Braithwaite, G. P.; Del Favero, P.; Skelton, B. W.; White, A. H. *Aust. J. Chem.* **1990**, *43*, 393.
(27) Haussühl, S. *Z. Kristallogr., Kristallgeom. Kristallphys., Kristallchem.* **1961**, *116*, 371.
(28) Beattie, J. K.; Best, S. P.; Del Favero, P.; Skelton, B. W.; Sobolev, A. N.; White, A. H. *J. Chem. Soc., Dalton Trans.* **1996**, 1481−1486.
(29) Cotton, F. A.; Fair, C. K.; Lewis, G. E.; Mott, G. N.; Ross, F. K.; Scultz, A. J.; Williams, J. M. *J. Am. Chem. Soc.* **1984**, *106*, 5319−5323.
(30) Tachikawa, H.; Ichikawa, T.; Yoshida, H. *J. Am. Chem. Soc.* **1990**, *112*, 977−982.
(31) Best, S. P.; Figgis, B. N.; Forsyth, J. B.; Reynolds, P. A.; Tregenna-Piggott, P. L. W. *Inorg. Chem.* **1995**, *34*, 4605−4610.
(32) Mabbs, F. E.; Machin, D. J. *Magnetism and Transition Metal Complexes*; Chapman and Hall: London, 1973.
(33) Best, S. P.; Armstrong, R. S.; Beattie, J. K. *J. Chem. Soc., Dalton Trans.* **1982**, 1655−1664.
(34) Best, S. P.; Beattie, J. K.; Armstrong, R. S. *J. Chem. Soc., Dalton Trans.* **1984**, 2611−2624.
(35) Beattie, J. K.; Armstrong, R. S.; Best, S. P. *Spectrochim. Acta* **1996**, *51A*, 539−548.
(36) Best, S. P.; Beattie, J. K.; Armstrong, R. S.; Braithwaite, G. P. *J. Chem. Soc., Dalton Trans.* **1989**, 1771−1777.
(37) Best, S. P.; Beattie, J. K.; Armstrong, R. S. *J. Chem. Soc., Dalton Trans.* **1992**, 299−304.
(38) Armstrong, R. S.; Beattie, J. K.; Best, S. P.; Cole, B. D.; Tregenna-Piggott, P. L. W. *J. Raman. Spectrosc.* **1995**, *26*, 921−927.

X-band EPR spectra were obtained using a Bruker 380e spectrometer. Samples doped with chromium(III) were made by cocrystallization of CsTiSH and $CsCr(SO_4)_2 \cdot 12H_2O$ in deoxygenated sulfuric acid (1 mol dm^{-3}). Single crystals were mounted on a perspex rod and sealed under a partial atmosphere of helium to assist conduction. The temperature of the cavity was monitored using a copper−constantine resistor.

Neutron time-of-flight powder diffraction data were collected on $CsTi(SO_4)_2 \cdot 12D_2O$ (CsTiSD) using the high-resolution powder diffractometer HRPD[39] at the ISIS spallation source. Approximately 5 g of CsTiSD single crystals were ground in a dry nitrogen atmosphere and loaded into an aluminium can of slab geometry, 1 cm thick, with thin vanadium front and back windows. Heat could be supplied directly using a cartridge heater placed in the side wall of the can; a Rh−Fe sensor was placed in the opposite wall. To avoid Bragg scattering from the can, sensor, and thermocouple, a thin gadolinium absorbing mask was screwed to the front of the can that faced the incident neutron beam and the high-resolution backscattering detectors. The screws were masked using thin cadmium foil. The sample was loaded into a standard, vanadium tailed ILL "orange" cryostat which permitted temperature control over the range 1.5−150 K. The powder data sets were background subtracted, normalized to the incident flux distribution, focused to a flight path of 95.9632 m at a 2θ of 168.33°, and finally corrected for detector efficiency. Data were collected in the time-of-flight range 30−130 ms, which corresponds to a d spacing range of 0.6−2.6 Å in the backscattering detectors. At a few temperatures some data sets were collected with a time-of-flight frame of 120−220 ms (2.4−4.4 Å) to study the temperature dependence of the low index Bragg reflections 004, 222, 220 in order to locate and characterize the nature of the phase transition. Data collection corresponding to 150 μAh of incident proton beam current were made at 1.6 and 20 K for crystal structure refinement of the low- and high-temperature modifications, respectively. The 120 μAh data collections were made at 50 and 100 K to further characterize the cubic phase. A number of short 20-μAh runs were made at 1 K intervals from 6 to 14 K, followed by runs at 16, 20, 30, 40, 60, and 80 K to follow the behavior of the unit cell parameters through the transition.

3. Results

HRPD. The powder data sets show that the Bragg peaks which index to the high-temperature cubic unit cell become split as the temperature is lowered to below 12 K indicating the presence of a structural phase transition (Figure 1). The temperature dependence of the diffraction pattern shows no evidence for hysteresis and is fully reversible. The line profiles were analyzed using a fully Bayesian approach.[40] Consideration of *hhh* and *hh*0 reflections suggested that the cell is metrically orthorhombic. The diffraction data at 1.6 K are found to be consistent with the orthorhombic space group *Pbca*, a subgroup of the β alum aristotype space group $Pa\bar{3}$. In the orthorhombic phase the site symmetry of $[Ti(OH_2)_6]^{3+}$ is lowered from S_6 to C_i.

The variation of the unit cell dimensions with temperature is shown in Figure 2. In the cubic phase the change in lattice constant with temperature follows a simple Einstein expression ($a = 12.40073 + 0.03089/(\exp(138/T) - 1)$). In the orthorhombic phase there is a significant increase in one of the cell parameters giving an overall increase in the unit cell volume on transforming from the cubic to the orthorhombic phase. To the precision of the data the phase transition is type II and continuous. The structure of the cubic phase of CsTiSD was solved using Rietveld methods at temperatures of 100, 50, and 20 K, using the program TF12LS,[41] on data collected over extended acquisition periods (≥120 μAh). The structures are in close agreement and a summary of the unit cell, data collection, and refinement parameters for the 20 K structure is given in Table 1. Atomic coordinates and structural parameters are presented in Tables 2 and 3, respectively. A table of unit cell parameters in the temperature range 100−1.44 K and a figure showing observed, calculated, and residual for the 20 K Rietveld refinement of CsTiSD are available as Supporting Information.

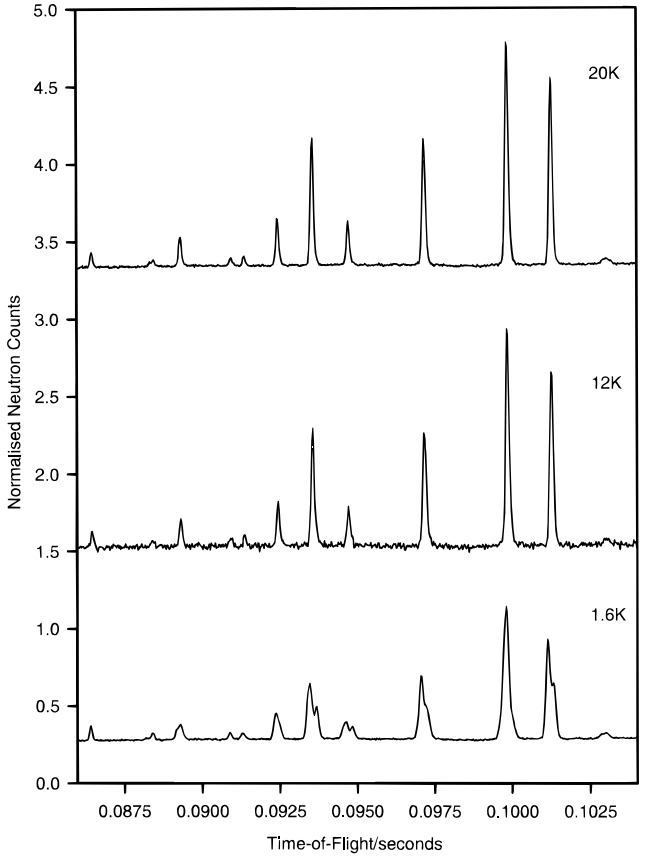

Figure 1. The powder neutron diffraction pattern of $CsTi(SO_4)_2 \cdot 12D_2O$ recorded using HRPD in backscattering geometry. The time-of-flight range (0.0860−0.1040 s) corresponds to a d spacing of 1.72−2.08 Å. Data collection was integrated over 150 (1.6 and 20 K) or 20 (12 K) μAh of incident proton beam current.

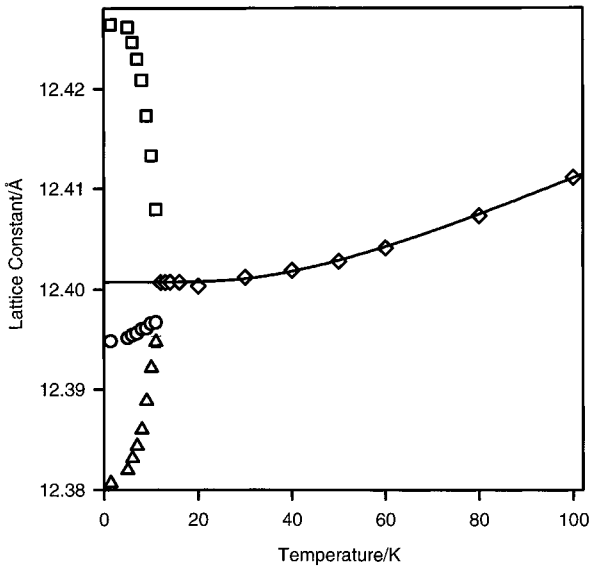

Figure 2. The temperature dependence of the unit cell dimensions of $CsTi(SO_4)_2 \cdot 12D_2O$ between 1.6 and 100 K; ◇ designates the unit cell dimension in the cubic space group $Pa\bar{3}$, and □, ○, and △ designate the unit cell dimensions in the orthorhombic space group *Pbca*.

(39) Johnson, M. W.; David, W. I. F. HRPD: The high resolution powder diffractometer at the SNS. RAL Report. RAL-85-112, 1985.
(40) Sivia, D. S.; Carlile, C. J. *J. Chem. Phys.* **1992**, *96*, 170−8.
(41) David, W. I. F.; Ibberson, R. M.; Matthewman, J. C. R. RAL Report. RAL-92-032, 1992.

Table 1. Crystal Data for the 20 K HRPD Structure Determination of $CsTi(SO_4)_2{\cdot}12D_2O$

formula	$CsTi(SO_4)_2{\cdot}12D_2O$
shorthand designation	CsTiSD
formula weight	612.9
space group	$Pa\bar{3}$
Z	4
temperature/K	20
a/Å	12.40081(1)
U/Å^3	1906.998(5)
D_{calcd}/g cm^{-3}	2.13
wavelength range/Å	0.6−4.4
data collection technique	time of flight Laue
no. of unique reflcns in final l.s.	1180
function minimized	$\sum w\|F_o - F_c\|^2$
R_p[a]	0.022
R_{wp}[b]	0.027
χ^2[c]	11.78

[a] $R_p = \sum|F_o - F_c|/\sum F_o$. [b] $R_{wp} = [\sum w|F_o - F_c|^2/\sum wF_o^2]^{1/2}$. [c] $\chi^2 = [\sum w(F_o - F_c)^2]/(N - P + C)$ where N is the number of observations, P is the number of variables, C is the number of constraints.

Table 2. Atomic Coordinates and Isotropic Temperature Factors from the 20 K HRPD Refinement of $CsTi(SO_4)_2{\cdot}12D_2O$

atom	x	y	z	B_{iso}
Cs	0.5	0.5	0.5	0.099(56)
Ti	0.0	0.0	0.0	0.193(83)
S	0.32738(22)	0.32738(−)	0.32738(−)	0.337(85)
O(1)	0.25793(14)	0.25793(−)	0.25793(−)	0.570(46)
O(2)	0.28082(14)	0.33427(14)	0.43645(13)	0.319(29)
O(a)	0.05362(16)	0.20722(16)	0.34241(14)	0.484(30)
D(a1)	0.01044(14)	0.22869(13)	0.28020(13)	1.328(33)
D(a2)	0.12724(15)	0.22032(14)	0.31788(14)	1.344(35)
O(b)	0.16332(14)	−0.00113(15)	−0.00021(15)	0.390(21)
D(b1)	0.21204(15)	−0.06102(14)	0.02303(14)	1.152(37)
D(b2)	0.20834(15)	0.06046(15)	−0.02347(13)	1.196(34)

The structural parameters derived from this analysis are in excellent agreement with those obtained from the 100 K X-ray structure of CsTiSH[42] (Table 3) although, as expected, there is significantly greater precision in the coordinates of the hydrogen (deuterium) atom positions using neutron techniques. The $[Ti(OD_2)_6]^{3+}$ cation is characterized by a TiO_6 framework which is little distorted from octahedral and the coordination geometry of O(b) is trigonal planar, *i.e.* the angle between the plane of the coordinated water molecule and the Ti−O(b) bond vector is 0.6(3)°. The angle between the plane of the coordinated water molecule relative to the TiO_6 framework, ϕ, has a value of −20.5(3)°, *i.e.* intermediate between that giving T_h symmetry ($\phi = 0°$) and *all-horizontal* D_{3d} ($\phi = -45°$), which is in close agreement with that obtained for caesium sulfate β alums ($-19° < \phi < -23°$). It is important to note that the hydrogen bonds involving the water molecule coordinated to M^{III} are relatively strong and linear (O−H···O ≈ 180°) and that independent of the hydrogen atom coordinates, the orientation of the water molecule coordinated to M^{III} can be estimated from the appropriate oxygen atom coordinates.[28] There is close agreement between the conformation of the water molecule coordinated to titanium(III) whether deduced from the hydrogen or oxygen atom coordinates, and in the latter case whether the X-ray or neutron structure is used.

For the low-temperature orthorhombic phase, the number of atoms in the asymmetric unit increases by a factor of 3, and due to the strong pseudosymmetry present in this phase, the structural parameters derived from Rietveld analysis have large estimated standard deviations compared to those determined in the cubic phase. In order to elucidate the structure of the low-temperature phase of CsTiSD, we have recently collected single-crystal data at 20 and 1.6 K using SXD at ISIS. The low-temperature crystal structure is currently being determined.

Table 3. Bond Lengths (Å) and Angles (deg) that Define the Coordination Environments in $CsTi(SO_4)_2{\cdot}12X_2O$

	HRPD, X = D	X-ray, X = H
	(i) SO_4^{2-}	
S−O(1)	1.492(3)	1.475(9)
S−O(2)	1.473(3)	1.484(4)
O(1)−S−O(2)	109.7(2)	109.6(2)
O(2)−S−O(2)	109.2(2)	109.3(2)
	(ii) $[Ti(OX_2)_6]^{3+}$	
Ti−O(b)	2.025(2)	2.028(5)
O(b)−Ti−O(b')	90.47(7)	90.3[a]
	(iii) Cs^+	
Cs−O(2)	3.497(2)	3.493(5)
Cs−O(a)	3.296(2)	3.314(5)
O(a)−Cs−O(a')	60.01(5)	60.0[a]
	(iv) Water Molecules	
O(a)−X(a1)	0.976(2)	0.875(149)
O(a)−X(a2)	0.976(3)	0.875(128)
O(b)−X(b1)	1.000(3)	0.976(122)
O(b)−X(b2)	0.989(3)	1.046(116)
H(a1)−O(a)−H(a2)	102.8(2)	89.5(9.5)
H(b1)−O(b)−H(b2)	108.5(2)	118.1(10.2)
	(v) Hydrogen bonds	
X(a1)···O(2)	1.810(3)	1.89[a]
X(a2)···O(1)	1.843(3)	1.98[a]
X(b1)···O(a)	1.606(3)	1.66[a]
X(b2)···O(2)	1.661(3)	1.60[a]
O(a)−X(a1)···O(2)	174.6(2)	173[a]
O(a)−X(a2)···O(1)	172.1(2)	158[a]
O(b)−X(b1)···O(a)	176.8(2)	162[a]
O(b)−X(b2)···O(2)	174.4(2)	169[a]

[a] Calculated from the atomic coordinates given in ref 40; note the different labeling scheme and error in sign of coordinates of Ow(2) (y/b should be −0.00024).

EPR Spectra of Cr^{3+}-Doped CsTiSH. The influence of the phase transition on the site of the tervalent cation has been examined by EPR spectra of chromium(III) doped into CsTiSH (Cs[Ti:Cr]SH). The concentration of chromium(III) in solution was *ca.* 0.01% of the total tervalent cation concentration. At this low dopant level it is presumed that the chromium(III) centers are homogenously distributed and do not significantly affect the structural chemistry of the host lattice. At temperatures above *ca.* 15 K, the EPR spectra of Cs[Ti:Cr]SH are in keeping with those of a wide range of chromium(III)-doped β alums.[43] Lines corresponding to the four chromium(III) cations per unit cell are found, each chromium(III) center being axially symmetric with the principal axis directed along a 3-fold axis of the unit cell. The value of the zero-field splitting parameter, D, was determined from spectral line positions when the external magnetic field was directed along the $\hat{\boldsymbol{z}}$ axis of the magnetic complex. In this instance, the spin Hamiltonian describing the spectrum is given by,

$$H_s = g_z \mu_B S_z B_z + D[S_z^2 - {}^1/_3 S(S+1)] \qquad (1)$$

At 15 and 298 K, D was determined to be $-532(5) \times 10^{-4}$ and $-590(5) \times 10^{-4}$ cm^{-1}, which are typical values for chromium(III) within the β alum lattice.[43] It is inferred, therefore, that from 298 to 15 K, CsTiSH shows no structural anomalies on the EPR time scale.

The temperature dependence of the single-crystal EPR spectra of Cs[Ti:Cr]SH, with the [100] direction of the crystal aligned closely with the external magnetic field, is shown in Figure 3. Along this direction, the principal axes of all four chromium-

(42) Sygusch, J. *Acta Crystallogr.* **1974**, *B30*, 662−665.

(43) Manoogian, A.; Leclerc, A. *J. Chem. Phys.* **1975**, *63*, 4450−4455.

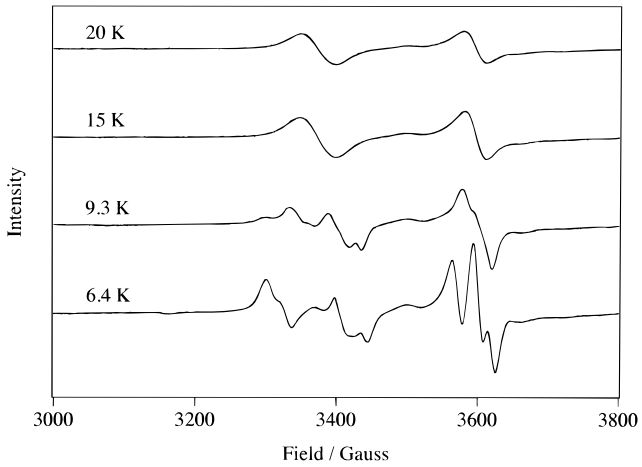

Figure 3. Variable-temperature EPR spectra of chromium(III)-doped $CsTi(SO_4)_2 \cdot 12H_2O$ with the field aligned along the [100] direction of the crystal.

(III) cations in the unit cell make the same angle with the magnetic field in the cubic phase. Two of the three allowed transitions are practically coincident being centered at 3374 G; the third transition occurs at 3598 G. The spectra recorded at 9.3 and 6.3 K show a clear splitting of all three EPR bands indicating that the chromium(III) centers are no longer magnetically equivalent at these temperatures. Although at present we have insufficient data to determine the spin Hamiltonian parameters, we have undertaken spectral simulations which show that the general appearance of the spectrum at 6.3 K can be reproduced only by assuming that, in addition to the nonequivalence of the four chromium(III) centers, they are no longer axially symmetric. The EPR spectra of chromium(III) doped into a range of lattices have been previously recorded down to 4.2 K and no such behavior has been noted.[43] Thus, the EPR results from Cs[Ti:Cr]SH must be interpreted in terms of a gross structural change of the host lattice between 15 and 9.3 K with an associated lowering of the site symmetry.

Single-Crystal Raman Spectra of $RbTi(SO_4)_2 \cdot 12H_2O$. The single-crystal Raman spectra of CsTiSH differ from those of the corresponding first-row transition metals and group 13 cations by the presence of an intense low-wavenumber band of E_g symmetry which shifts to lower wavenumber on cooling.[34,44] The wavenumbers of several other bands in the spectrum also show sensitivity to temperature.[34] The unusual temperature dependence of the half widths and wavenumber of these bands has been related to the phase transition of CsTiSH,[34] this being supported by the discontinuous spectral changes which occur on cooling below the transition temperature.[44] Polarized single-crystal Raman spectra of RbTiSH have been reported and assigned over the wavenumber range 275−1200 cm^{-1} at 80 K.[21] Bands found in this region comprise the internal modes of $[Ti(OH_2)_6]^{3+}$ and sulfate and the external modes of coordinated water. The spectra confirm classification of RbTiSH to the β alum modification,[21] isostructural with CsTiSH but atypical of the rubidium sulfate alums in general. In common with CsTiSH, the mid-wavenumber Raman spectra at 80 K show a pronounced broadening of several of the bands of E_g symmetry. In particular, the external modes of water coordinated to titanium(III) give band profiles with greatly increased half widths and wavenumbers which are in poor agreement with expectations based on the spectra of related β alums.[21,34] The low-wavenumber unpolarized spectra of RbTiSH over the temperature range 190 to 4 K are shown in Figure 4. Bands found in this region comprise the internal modes of $[Rb(OH_2)_6]^{+}$ and the external modes of the constituent ions. The spectra are dominated by an intense band which shifts from 40 cm^{-1} at 200 K to 22 cm^{-1} on cooling to 15 K but which exhibits a marked reduction in half width and an increase in wavenumber on further cooling. Splittings are evident for several higher wavenumber bands in spectra recorded below 10 K. The Raman spectra of RbTiSH are remarkably similar to those found for CsTiSH both in terms of the band profiles and their wavenumber dependence on temperature. The relationship between the Raman spectra and the phase transition of CsTiSH has been characterized by a range of spectroscopic and structural techniques and on this basis the spectral changes observed for RbTiSH are interpreted in terms of an analogous phase transition of the rubidium salt.

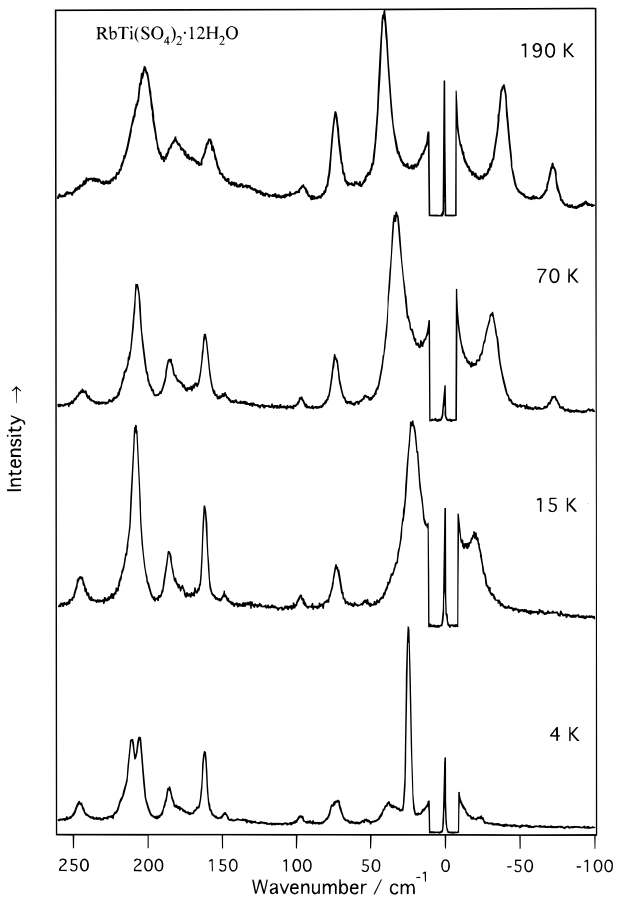

Figure 4. Raman spectra of a randomly oriented single crystal of $RbTi(SO_4)_2 \cdot 12H_2O$ at 4, 15, 70, and 190 K (step size 0.4 cm^{-1}; spectral bandwidth 2.93 cm^{-1} at 75 cm^{-1}; integration time 2 s; 25-mW, 413-nm radiation at sample). The laser was attenuated when scanning close to the exciting line.

4. Discussion

The structural instability of CsTiSH and RbTiSH is not exhibited by any of the rubidium or caesium sulfate alums of the wide range of tervalent cations examined to this time (Al,[21,33] Ga,[21,34] In,[21,34] V,[21,34] Cr,[21,34] Fe,[21,34] Co,[37] Mo,[38] Ru,[38] Rh,[36] and Ir[37]). A low-wavenumber band of E_g symmetry of $CsRu(SO_4)_2 \cdot 12H_2O$ has been reported to shift to lower wavenumber on cooling to 60 K;[23] however, no other anomalies in the vibrational spectra[38] or the 15 K neutron structures of the hydrate[23] and deuterate[25] salt are apparent. It is unlikely that the structural instability of the titanium alums is due to the size of the tervalent cation since the ionic radius of titanium(III) is intermediate between that of aluminium(III) and indium(III).[4]

(44) Armstrong, R. S. Private communication.

Hence the electronic structure of $[Ti(OH_2)_6]^{3+}$ is implicated. The principal interactions which can act to lift the degeneracy of the $^2T_{2g}$ (O_h) term in the alum lattice are the trigonal field, the JT effect, and spin−orbit (SO) coupling. The resulting electronic structure will depend on the relative strengths of these interactions. The magnitude of the trigonal field will depend on the orientation of the coordinated water molecule relative to the MO_6 axes and the relative magnitudes of the metal−water π interaction in and normal to the plane of the ligand.[24,45] The orientation of the water molecule coordinated to titanium(III) is in close agreement with that of the β alums,[24] including vanadium,[46] and it is reasonable to assume that the relative magnitudes of the π interaction in and normal to the plane of the water would be similar for titanium and vanadium and thus, the ordering of the energies of the a_g and e_g (S_6) orbitals will be the same. For vanadium(III) in the β alum lattice, low-temperature magnetochemical measurements have established unambiguously that the ^3A_g trigonal term is lower lying with a zero-field splitting of 4.95 cm^{-1}.[16] The electronic Raman transition of the vanadium alums enables a quantification of the trigonal field splitting, this having a value of *ca.* 1950 cm^{-1}.[19,21] The electronic structure of vanadium(III) within the β alum lattice has been interpreted in terms of the trigonal field being the principal interaction acting upon the $^3T_{2g}$ (O_h) term with the effects of SO coupling and vibronic coupling treated as perturbations to the trigonal field terms.[20,21] While the analogous intra-t_{2g} electronic Raman transition of titanium(III) has yet to be identified, the trigonal field splitting of the $^2T_{2g}$ (O_h) ground term is predicted to be of at least the same magnitude as that found for $[Ti(OH_2)_6]^{3+}$, resulting in a ground term which is orbitally degenerate (^2E_g) with the ^2A_g term relatively high in energy.

The ^2E_g (S_6) ground term of titanium(III) will be subject to JT and SO coupling, with the JT coupling restricted to phonon modes of E_g symmetry. This is reflected in the Raman spectra of CsTiSH[34] and RbTiSH[21] which are marked by the anomalously large half widths of a number of the E_g bands. In particular, the profiles of the bands associated with the librational modes of water coordinated to titanium(III) are broad and indistinct, a feature commonly associated with dynamic distortion of the water molecules,[47] with band wavenumbers which are highly irregular compared with those of other β hydrate alums. The low-wavenumber lattice mode has a pronounced temperature dependence suggesting that this mode is strongly associated with the phase transition. Assignments of the lattice modes of the caesium alums have been reported,[35] these being based on shifts observed on sulfate/selenate exchange, deuteration, and isomorphous replacement of the tervalent cation. The lowest wavenumber band of E_g symmetry occurs between 52 and 59 cm^{-1} and is sensitive both to deuteration and to substitution of selenate for sulfate and has been assigned to a mode involving translation of the anion and a motion of the water molecules or complex cations. The relationship between the sulfate groups and the orientation of the water molecule coordinated to the tervalent cation is shown in Figure 5. The sulfate groups provide the most direct link between the titanium(III) centers in the crystal and librations of the anion provide a means by which an interaction between the $[Ti(OH_2)_6]^{3+}$ can occur, ultimately resulting in an ordering of the JT distortions of the titanium(III) hexaaqua cations, *i.e.* a cooperative Jahn-Teller effect (CJTE).

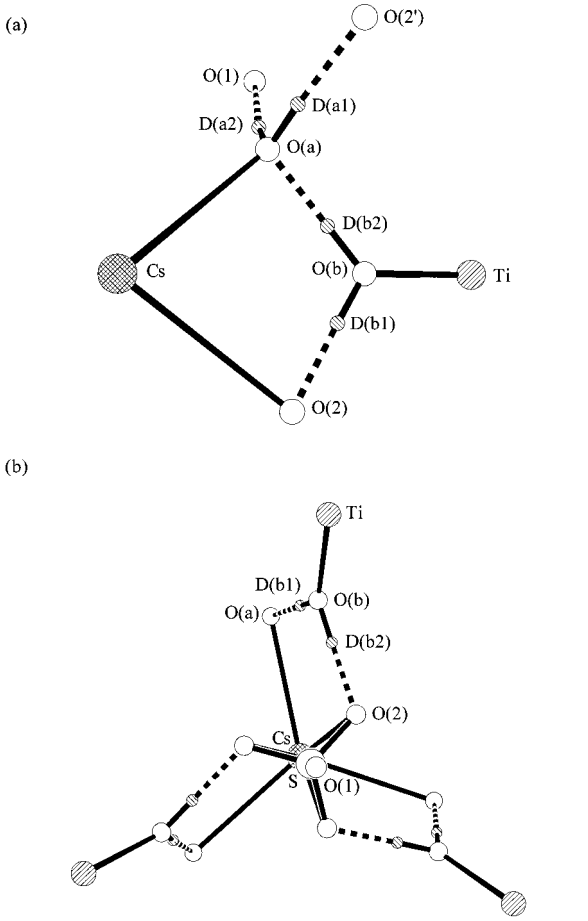

Figure 5. Details of the structure of $CsTi(SO_4)_2 \cdot 12D_2O$ showing (a) the disposition of the hydrogen bonding arrangement of the asymmetric unit and (b) a view down the 3-fold axis of the cell showing the disposition of the titanium(III) cations relative to the sulfate group (for clarity, D(a1) and D(a2) are not shown).

The CJTE is a phase transition resulting from the correlation of JT centers within a crystal. At sufficiently high concentrations, the influence of surrounding JT centers will act to lift the degeneracy of equivalent JT distortions of an isolated molecule. The correlation between the JT centers may occur in a number of different ways giving rise to configurations of different energies. Below a critical temperature, the distortions of the JT centers will be locked into the most favorable configuration as the crystal adopts the structure of minimum free energy. The JT centers are then, in effect, subject to a crystal field of lower symmetry. Above the critical temperature, the thermal energy available to the system tends to destroy the correlation and the motion of each JT center preserves, dynamically, the point symmetry in the high-temperature phase. The CJTE is now recognized as an integral part of solid state chemistry and is discussed comprehensively in the literature.[48,49]

The transition temperature of the CJTE largely depends on the strength of the interaction between the localized degenerate electronic orbitals and the phonon modes of the crystal lattice. For transition metal ions with unequal occupancy of the e_g (O_h) orbitals, which are metal−ligand σ antibonding in character, there is a strong vibronic interaction reflected by a high CJTE

(45) Daul, C.; Goursot, A. *Inorg. Chem.* **1985**, *24*, 3554−3558.
(46) Beattie, J. K.; Best, S. P.; Moore, F.; White, A. H. *Aust. J. Chem.* **1993**, *46*, 1337−1345.
(47) Tanaka, H.; Henning, J.; Lutz, H. D.; Kliche, G. *Spectrochim. Acta* **1987**, *43A*, 395. Eckers, W.; Lutz, H. D. *Spectrochim. Acta* **1985**, *41A*, 1321. Frindi, M.; Peyrard, M.; Remoissenet, M. *J. Phys.* **1980**, *C13*, 3493.
(48) Kaplan, M. D.; Vekhter, B. G. *Cooperative phenomena in Jahn-Teller crystals*; Plenum Press: New York, 1995. Bersuker, I. B. *The Jahn-Teller Effect and Vibronic Interactions in Modern Chemistry*; Plenum Press: New York, 1984. Englman, R. *The Jahn-Teller Effect in Molecules and Crystals*; Wiley: London, 1972.
(49) Gehring, G. A.; Gehring, K. A. *Coop. Jahn-Teller Effects, Rep. Prog. Phys.* **1975**, *38*, 1−89.

Table 4. Selection of Published *g* Values of Titanium(III) in $CsTi(SO_4)_2 \cdot 12H_2O$

temp range, K	technique	*g* values	ref
80−300	magnetic susceptibility	$g_{\|\|} = 1.88$ $g_\perp = 1.62$	8
100−300	magnetic susceptibility	$g_{\|\|} = 1.92$ $g_\perp = 1.78$	7
1−4.2	magnetic susceptibility	$g_{eff} = 1.12$	5
2.5−4.2	EPR	$g_{\|\|} = 1.25$ $g_\perp = 1.14$	6, 52

transition temperature, *e.g.* the $(t_{2g})^3(e_g)^1$ cation Mn^{3+} in the spinel Mn_3O_4 has a transition temperature of 1170 K.[50] Examples of weak coupling are provided by the rare earth zircons which have the general formula RXO_4 where R is a tervalent lanthanide ion and X is V, As, or P. Certain members of this group undergo CJTE with a transition temperature close to that of liquid helium.[49] The low transition temperature reflects the weak interaction between the JT electrons, which lie in the highly shielded 4f orbitals, and the crystal lattice. In the titanium alums the JT electrons lie in orbitals which are nonbonding/π antibonding in character, also resulting in a weak interaction with the crystal lattice. In addition the ^2E_g ground term is split to first order by SO coupling which competes with the JT splitting. These factors, along with the large separation of titanium(III) centers within the lattice ($r_{Ti-Ti} = 8.769$ Å at 20 K), contribute to the low transition temperature.

Reinterpretation of the *g* Values of CsTiSH. The *g* values of CsTiSH have been a subject of study and contention since the early development of crystal field theory. The EPR spectrum can be observed only at temperatures approaching that of liquid helium where it is broad and indistinct.[6,51,52] Furthermore, susceptibility measurements of CsTiSH in the cubic phase do not permit determination of the magnetic anisotropy.[7,8,10] These factors have led workers to make fundamental assumptions as to the electronic structure of the $[Ti(OH_2)_6]^{3+}$ cation within the alum lattice with numerous models proffered.[1,5−14]

A summary of some of the *g* values reported for CsTiSH is presented in Table 4. The *g* values obtained from EPR[6,52] are determined directly and are likely to be the most reliable. Between 1 and 4.2 K, the susceptibility is reported to obey Curie's law[5] and calculation of the effective *g* value follows directly from the Curie constant. Susceptibility measurements undertaken above 4.2 K show a complicated variation with temperature.[7−10] The *g* values quoted in this temperature range are calculated indirectly using values of crystal field parameters that are found to best fit the data.

The discrepancy between the *g* values determined from measurements made below 4.2 K and those calculated from measurements above 80 K has yet to be adequately explained. It has been suggested that the trigonal field splitting must be reduced drastically on cooling in order to account for the discrepancy in the *g* values.[7] A model which takes into account second-order contributions from the cubic ^2E_g term and anisotropic orbital reduction factors has been found to give good agreement with the observed *g* values but not with a unique set of parameters. In addition, no set of parameters from this analysis were found that could reproduce the variation of the magnetic moment with temperature in the 80−300 K temperature range.[9]

The analysis of the electronic structure of titanium(III) in CsTiSH has been based on the assumption that the sign of the trigonal field is such as to give an orbitally nondegenerate ground term, contrary to that which follows from considerations of the molecular structure of the cation. This assumption may be understood by consideration of the magnetic properties of the ground Kramers doublet which results from the $^2T_{2g}$ term after perturbation by SO coupling and an axial crystal field.[32] If the $[Ti(OH_2)_6]^{3+}$ cation is axially symmetric then a ^2E_g ground term would result in a ground state Kramers doublet with wavefunctions represented by $\psi_{m_l=1}^{m_s=-1/2}$, $\psi_{m_l=-1}^{m_s=1/2}$ where m_s and m_l refer to the projection of the spin and effective orbital angular momenta on the $\hat{\mathbf{z}}$ axis. Since the spin and orbital angular momentum are equal and opposite, a first-order Zeeman splitting along the $\hat{\mathbf{z}}$ direction can be observed only on account of a reduction of orbital angular momentum. Upon operating with the magnetic moment operator in the $\hat{\mathbf{x}}\hat{\mathbf{y}}$ plane all matrix elements are zero so that $g_\perp = 0$. The experimental values of $g_{\|} = 1.25$ and $g_\perp = 1.14$ have therefore been used to exclude the possibility of a ^2E_g trigonal ground term. However, this conclusion is valid only if the $[Ti(OH_2)_6]^{3+}$ cation is not subject to dynamic or static distortions. For example, the magnetic properties of the ^2E_g ground term subject to linear JT coupling will be modified by a quenching of the operators governing spin−orbit coupling and the orbital Zeeman interaction.[53] This will result in a decrease in the effective orbital angular momentum beyond that attributable to covalent bonding. A finite first-order Zeeman splitting in the perpendicular direction can also occur if the lattice strain, which causes the symmetry of the complex to be lowered, is strong enough.[54] This is most readily achieved when the JT coupling is of a cooperative nature.

Below the temperature of the phase transition the $[Ti(OH_2)_6]^{3+}$ centers are locked into one of the three possible distortion correlated minima. Since E_g phonon modes displace the $[Ti(OH_2)_6]^{3+}$ ions along coordinates which preserve the local C_i symmetry, the JT interaction cannot remove the inversion center. In view of the low symmetry distortion, an approximate calculation of the *g* values can be made as follows: We take as a basis just the E doublet states, and ignore any admixture of the d_{z^2} orbital by the trigonal field. The effect of the static low-symmetry distortion is represented as the non-zero value of one of the JT active coordinates. In the presence of a magnetic field **B**, the energies of the eigenstates are then represented by the eigenvalues of the matrix,

$$\begin{array}{c} \\ \psi_{m_l=1}^{m_s=-1/2} \\ \psi_{m_l=1}^{m_s=1/2} \\ \psi_{m_l=-1}^{m_s=-1/2} \\ \psi_{m_l=-1}^{m_s=1/2} \end{array} \begin{array}{c} \begin{array}{cccc} \psi_{m_l=1}^{m_s=-1/2} & \psi_{m_l=1}^{m_s=1/2} & \psi_{m_l=-1}^{m_s=-1/2} & \psi_{m_l=-1}^{m_s=1/2} \end{array} \\ \begin{bmatrix} (p-1)B_z & B_x + iB_y & VQ & 0 \\ B_x - iB_y & \lambda + (p'+1)B_z & 0 & VQ \\ VQ & 0 & \lambda - (p'+1)B_z & B_x + iB_y \\ 0 & VQ & B_x - iB_y & (1-p)B_z \end{bmatrix} \end{array} \tag{2}$$

where p and p' are reduction factors that approximately represent the effect of the JT interaction together with any reduction of the orbital angular momentum by the bonding, λ is the spin−orbit splitting, V is the JT coupling constant, and Q is the static distortion of one normal coordinate. The Bohr magneton is absorbed into **B**.

In the absence of a magnetic field the energies are,

$$E = {}^1/_2(\lambda \pm \sqrt{\lambda^2 + 4(VQ)^2}) \tag{3}$$

The *g* values are obtained by finding the eigenvalues of this

(50) Aoki, I. *J. Phys. Soc. Jpn.* **1962**, *17*, 53−61.
(51) Bijl, D. *Proc. Phys. Soc. A* **1950**, *63*, 407.
(52) Harrowfield, B. V. *Phys. Abstr.* **1972**, *75*, 594, No. 10288.
(53) Ham, F. S. *Phys. Rev.* **1965**, *138*, A1727. Ham, F. S. *Phys. Rev.* **1968**, *166*, 307.
(54) Dubiki, L; Riley, M. J. *J. Chem. Phys.* **1997**, *106*, 1669.

matrix and expanding them to first order in B_x, B_y, or B_z. The coefficients of B_x and B_y are identical so a local distortion along a JT coordinate does not remove the axial symmetry of the g tensor. In the lower doublet,

$$g_{\parallel} = 2 - p + p' - \frac{(p + p')\lambda}{\sqrt{\lambda^2 + 4(VQ)^2}} \quad (4)$$

$$g_{\perp} = \frac{4VQ}{\sqrt{\lambda^2 + 4(VQ)^2}} \quad (5)$$

The predicted axial symmetry follows from the assumption that the low-symmetry distortion is along a JT active coordinate as this yields the greatest electronic stabilization. Strains of other symmetries would introduce extra terms to the Hamiltonian and so may allow g_x and g_y to take different values.

The EPR spectra of Ti^{III} in CsTiSH between 2.5 and 4.2 K suggest the **g** tensor to be axially symmetric with $g_{\parallel} = 1.25$ and $g_{\perp} = 1.14$. The latter result gives $2VQ/(\lambda^2 + 4(VQ)^2)^{1/2} = 0.57$ whence $\lambda/(\lambda^2 + 4(VQ)^2)^{1/2} = 0.82$, and so this simple model predicts $p = 0.41 + 0.10p'$. We note that the magnetic properties of the ground state Kramers doublet are similar to those of platinum in silicon occupying a negatively charged lattice vacancy.[55] It was noted that the **g** tensor will remain nearly axially symmetric as long as the axial field is large enough so that spin−orbit coupling to the nondegenerate axial term is small. This situation pertains to $[Ti(OH_2)_6]^{3+}$ in the alum lattice.

The conclusion that the ground state g values arise from a low-symmetry distortion of $[Ti(OH_2)_6]^{3+}$ has also been realized by Dubicki and Riley.[54] These workers have undertaken exact calculations of the linear $^2T\otimes\epsilon$ coupling with the coupling strength, trigonal field, and low-symmetry strain parameters as variables. It is shown that for a trigonal field of the magnitude as that found in the β alums, the trigonal field breaks the $^2T\otimes\epsilon$ coupling into $^2E\otimes\epsilon$ and $^2A\otimes\epsilon$ as assumed in our analysis. This work provides detailed insight into the anomalous fine structure observed in the EPR spectrum of titanium(III) as an impurity in the β alums. With the JT active mode assumed to be the $\nu_2(TiO_6)$ skeletal stretch, occurring at *ca.* 450 cm^{-1}, the ground state g values could be reproduced assuming a strain splitting of 56 cm^{-1}. Likewise, good agreement with the ground state g values for CsTiSD ($g_{\parallel} = g_{\perp} = 1.31$)[52] could be found by increasing the strain splitting to 70 cm^{-1}, all other parameters remaining constant. However, the values of the strain splittings obtained depends on the other parameters employed and the assumption that the JT interaction is dominated by coupling to the $\nu_2(TiO_6)$ mode. This assumption is supported neither by the Raman spectra nor by simple considerations of the electronic structure of $[Ti(OH_2)_6]^{3+}$. The energy of the first excited vibronic state, calculated to be >60 cm^{-1}, is in poor agreement with the value of 21.3 cm^{-1} implied by Raman measurements on titanium(III)-doped $CsAl(SO_4)_2 \cdot 12H_2O$.[56] Additionally, no account has been taken of the decrease in the phonon frequency upon deuteration, resulting from an increase in the effective mass of the phonon mode. This gives rise to a lowering of the zero-point energy of the JT-active mode which generally leads to a greater quenching of orbital angular momentum.

Recently much attention has been paid to cooperative phenomena in a variety of copper(II) salts where the structural parameters typically show a marked temperature dependence, which can be rationalized in terms of Boltzmann averaging of vibronic states localized in different potential minima.[57,58] The situation contrasts to that of titanium(III) where, in addition to the JT interaction being substantially weaker, the ^2E_g ground term is split to first order by spin−orbit coupling. As a result the potential energy surface for titanium(III) in CsTiSH will differ considerably to that of copper(II) in $(NH_4)_2[Cu(OH_2)_6](SO_4)_2$ in that distinct potential minima are not formed so that for CsTiSH the concept of fluxional behavior between different structures is not valid.

5. Conclusion

The electronic structure of $[Ti(OH_2)_6]^{3+}$ within CsTiSH has been a source of contention for over 40 years with previous models all based on the presumption that CsTiSH is structurally well-behaved over the whole experimental temperature range. The ground state g values of $g_{\parallel} = 1.25$ and $g_{\perp} = 1.14$ have then been used to exclude the possibility of the trigonal field being of a sign such that the E_g term is lowest lying, since, within the confines of crystal field theory, the ground Kramers doublet is non-magnetic with $g_{\perp} = 0$. In this work we have shown that CsTiSH is subject to a phase transition at *ca.* 12 K which we associate with a CJTE, and that similar structural chemistry is suggested for RbTiSH. In the context of the phase transition, the ground state g values may be readily explained assuming that the ^2E_g trigonal term is lower lying. The low-symmetry crystal field mixes the two Kramers doublets arising from the ^2E_g trigonal term giving rise to a finite first-order Zeeman splitting in the perpendicular direction. It is important to emphasize that the JT distortion while reducing the symmetry of the complex leaves $g_x = g_y$ so that the **g** tensor remains axially symmetric irrespective of the magnitude of the distortion.

The g values determined for CsTiSH from susceptibility measurements between 80 and 300 K[7,8] have no relevance since they were determined indirectly from a highly parametrized crystal field model which assumes a nondegenerate trigonal ground term. Indeed, employing the same degree of parametrization, we have obtained an equally good fit of the same data set using a crystal field model with a ^2E_g ground term.[59] Since there is a gross distortion of $[Ti(OH_2)_6]^{3+}$ resulting from the phase transition at 12 K, a different set of parameters will apply in different experimental temperature ranges. Therefore, a meaningful comparison between g values obtained from susceptibility measurements and those from EPR measurements can only be made when the EPR measurements are on dilute samples which are structurally stable over the temperature range of the measurement. To this extent we have undertaken an extensive EPR and magnetic susceptibility study of CsTiSH both as the pure alum and diluted into a range of diamagnetic β-alum hosts. We have found that all the data over the whole experimental temperature range can be explained within a self-consistent model as outlined in this paper. The results of this study are currently being prepared for publication.

(55) Anderson, F. G.; Ham, F. S.; Watkins, G. D. *Phys. Rev. B* **1992**, *45*, 3287−3303.

(56) Chase, L. L.; Glynn, T. J.; Hayes, W.; Rushworth, A. J.; Ryan, J. F.; Walsh, D.; De Goer, A. M. *Proceedings of the Fifth International Conference on Raman Spectroscopy*, Freiburg, Germany, 1976; Schmid, E. D., Brandmueller, J., Kiefer, W., Eds.; Hans Ferdinand Schulz Press, 1976; pp 660−661.

(57) Hathaway, B. J.; Hewat, A. W. *J. Solid State Chem.* **1984**, *51*, 364. Alcock, N. W.; Duggan, M.; Tyagi, S.; Hathaway, B. J.; Hewat, A. W. *J. Chem. Soc., Dalton Trans.* **1984**, 7. Stebler, M.; Bürgi, H. B. *J. Am. Chem. Soc.* **1987**, *109*, 1395. Simmons, C. J.; Hathaway, B. J.; Amornjarusiri, K.; Santasiero, B. D.; Clearfield, A. J. *J. Am. Chem. Soc.* **1987**, *109*, 1947. Rauw, W.; Ahsbahs, H.; Hitchman, M. A.; Lukin, S.; Reiner, D.; Schultz. A. J.; Simmons. C. J.; Stratemeier. H. *Inorg. Chem.* **1996**, *35*, 1902.

(58) Simmons, C. J.; Hitchman, M. A.; Stratemeier, H.; Schultz, A. *J. Am. Chem. Soc.* **1993**, *115*, 11304−11311.

(59) Tregenna-Piggott, P. L. W. Ph.D. Thesis, London, 1994.

Acknowledgment. We thank Professor R. S. Armstrong for Raman spectra of CsTiSH over the temperature range 10−80 K, Drs. L. Dubicki and M. Riley for helpful discussions and a preprint of their manuscript prior to publication, Høgni Weihe and Chris Noble for the use of their EPR simulation software, Professor R. J. H. Clark and the University of London Intercollegiate Research Service for access to the Raman spectrometers, the Research Corporation Trust for the purchase of the MD4 cryostat, and the SERC for providing access to the neutron sources. PLWT-P thanks the Royal Society for the award of a fellowship to undertake research in this area.

Supporting Information Available: Table of unit cell parameters in the temperature range 100−1.44 K, observed, calculated, and residual data for the 20 K Rietveld refinement of $CsTi(SO_4)_2 \cdot 12D_2O$, and EPR simulations showing how the general form of the EPR spectra of Cs[Ti:Cr]SH as a function of temperature (Figure 3) may be reproduced as a result of a lowering of the crystal and site symmetries (4 pages). See any current masthead page for ordering and Internet access instructions.

JA963509W